A field study of reflectivity and Z-R relations using vertically pointing radars and disdrometers

A Field Study of Reflectivity and *Z–R* Relations Using Vertically Pointing Radars and Disdrometers

ALI TOKAY

Joint Center for Earth Systems Technology, University of Maryland, Baltimore County, Baltimore, and NASA Goddard Space Flight Center, Greenbelt, Maryland

PETER HARTMANN AND ALESSANDRO BATTAGLIA

Meteorological Institute, The University of Bonn, Bonn, Germany

KENNETH S. GAGE, WALLACE L. CLARK, AND CHRISTOPHER R. WILLIAMS

Cooperate Institute for Research in Environmental Sciences, University of Colorado, and NOAA/Earth System Research Laboratory, Boulder, Colorado

(Manuscript received 5 May 2008, in final form 11 December 2008)

ABSTRACT

Observations from a 16-month field study using two vertically pointing radars and a disdrometer at Wallops Island are analyzed to examine the consistency of the multi-instrument observations with respect to reflectivity and *Z–R* relations. The vertically pointing radars were operated at S and K bands and had a very good agreement in reflectivity at a gate centered on 175 and 177 m above ground level over a variety of storms. This agreement occurred even though the sampling volumes were of different size and even though the S band measured the reflectivity factor directly, whereas the K-band radar deduced it from attenuated K-band measurements. Indeed, the radar agreement in reflectivity at the collocated range gates was superior to that between the disdrometer and either radar. This is attributed in large part to the spatial separation of the disdrometer and radar sample volumes, although the lesser agreement observed in a prior collocated disdrometer–disdrometer comparison suggests the larger size of the radar sample volumes as well as the better overlap also play a role. Vertical variations in the observations were examined with the aid of the two radar profilers. As expected, the agreement between the disdrometer reflectivity and the reflectivity seen in the vertically pointing radars decreased with height. The effect of these vertical variations on determinations of *Z–R* relation coefficients was then examined, using a number of different methods for finding the best-fitting coefficients. The coefficient of the *Z–R* relation derived from paired disdrometer rain rate and radar reflectivity decreased with height, while the exponent of the *Z–R* relation increased with height. The coefficient and exponent of the *Z–R* relations also showed sensitivity to the choice of derivation method [linear and nonlinear least squares, fixed exponent, minimizing the root-mean-square difference (RMSD), and probability matching]. The influence of the time lag between the radar and disdrometer measurements was explored by examining the RMSD in reflectivity for paired measurements between 0- and 4-min lag. The no-lag conditions had the lowest RMSD up to 400 m, while 1-min lag gave the lowest RMSD at higher heights. The coefficient and exponent of the *Z–R* relations, on the other hand, did not have a significant change between no-lag- and 1-min-lag-based pairs.

1. Introduction

Measurements made by diverse instruments often are separated in time and/or space. In radar meteorology the time–height ambiguity is one of the major causes for uncertainty in the relationship between the radar-measured reflectivity Z and surface rain rate R. Even for a well-calibrated radar in the absence of partial beam-filling effects, drop sorting, the deviation of the hydrometeors trajectory from its vertical axis, and sampling volume differences are three major sources for the mismatch between radar and in situ rain estimates

Corresponding author address: Ali Tokay, NASA Goddard Space Flight Center, Code 613.1, Greenbelt, MD 20771.
E-mail: ali.tokay-1@nasa.gov

DOI: 10.1175/2008JTECHA1163.1

(Lee and Zawadzki 2005). While surface-based rain measuring devices are also subject to intrinsic measurement errors (e.g., Habib et al. 2001b; Ciach 2003; Tokay et al. 2005), these are thought to be small compared to the factors mentioned above.

Knowledge of the ambient hydrometeor size distributions is essential to overcome this time–height ambiguity. Vertically pointing radars measure vertical profiles of the integral parameters of the size distribution including reflectivity and, therefore, are invaluable in filling the gap between scanning radars and in situ rain measuring devices (Gage et al. 2000). In this paper, we compare observations simultaneously obtained using a collocated disdrometer, an S-band vertically pointing radar, also known as a profiler, and a vertically pointing K-band micro rain radar (MRR).

During the National Aeronautics and Space Administration's (NASA) Tropical Rainfall Measuring Mission (TRMM) field campaigns, a 915-MHz profiler and an impact-type Joss–Waldvogel (JW) disdrometer operated side by side near Houston, Texas, and near Melbourne, Florida, for two-month periods in spring and autumn 1998, respectively. Time series of profiler-measured and disdrometer-calculated reflectivity tracked each other quite well (Gage et al. 2000). Considering that the profiler's lowest reliable gates were centered 327 and 422 m above the ground, the agreement between the two instruments was quite reasonable. Later, Williams et al. (2005) showed a reflectivity-dependent bias in Florida where the selected profiler pulse volume was centered at 308 m above the ground. The reflectivity-dependent bias between profiler and disdrometer measurements was not site dependent. Clark et al. (2005) confirmed the bias between the two measurements in coincident datasets in Ji-Paraná, Brazil, and Kwajalein, Republic of Marshall Islands, where the selected profiler's gates were centered at 304 and 519 m, respectively.

To further investigate the differences between profiler and disdrometer reflectivities, an S-band profiler was operated next to a JW disdrometer at NASA's Wallops Flight Facility (WFF), Wallops Island, Virginia. Improving on previous field campaigns, the profiler's lowest reliable gate was centered at 146 m (second gate). This setup was designed to close the gap between the profiler and disdrometer observations, and the reflectivity-dependent bias between the profiler and the disdrometer reflectivities was substantially improved (Clark et al. 2005). These early results suggest that the time–height ambiguity is indeed the main factor accounting for discrepancies between the profiler and disdrometer measurements.

In addition to the S-band profiler, WFF is hosting vertically pointing K-band radar, also known as the MRR, on loan from Metek GmbH, Germany. Considering that the MRR's lowest reliable gate was centered at 70 m (second gate), drops of 0.5- and 5-mm diameter with 2 and 9 m sec^{-1} terminal fall speeds, respectively, will reach the ground with a time difference of 27 ± 7 s. For the lowest reliable gate of the S-band profiler, the time difference was 57 ± 6 s. This example shows the potential use of MRR to further reduce the gap between the profiler and disdrometer measurements. It should be noted that neither vertically pointing radars nor disdrometers are operational tools. The operational radar rainfall estimation relies on scanning radars and rain gauges. As a reference, the second lowest gates of the MRR and S-band profiler correspond to 9.3- and 18.1-km distance, respectively, for the lowest tilt (0.5°) of the National Weather Service's (NWS) Weather Surveillance Radar-1988 Doppler (WSR-88D).

The primary objective of this study is to investigate the vertical variability of radar-measured reflectivity Z and the *Z–R* relations found for each height using the reflectivity Z-measured aloft matched to the surface disdrometer–measured rain rate *R*. The comparisons were carried out for a variety of storms, ranging from summertime convective showers and remnants of tropical cyclones to cold and warm frontal rainfall. As a preliminary step, a detailed comparison of reflectivity measurements is performed between the two vertically pointing radars and the disdrometer. Prior to the presentation of our findings, we briefly describe the measurement site and the instruments in section 2, while the rainfall statistics are presented in section 3. Comparisons of event totals for two tipping-bucket rain gauges and a disdrometer can be found in section 4. The comparison of reflectivity measurements between vertically pointing radars and between radar and disdrometer for each event are presented in section 5. We further examine the correlations, biases, and standard deviations between disdrometer and radar reflectivity measurements for each range gate of the radars within a kilometer above the ground. The variability of the *Z–R* relation is then presented for each range gate of the profiler and MRR in section 6. The sensitivity of the *Z–R* relations to the method of derivation is considered in section 7. The role of the time lag between the radar and disdrometer measurements is also examined for completeness. Summary and conclusions are presented in the last section. It should be noted that we often use the term *radar* to refer to both the profiler and to the MRR throughout the manuscript, although *profiler* is used only to refer to the S-band vertically pointing radar.

2. Measurement site and instruments

Supported by the NASA TRMM satellite validation program, an in situ rain-measuring instrument test bed

has been operating at WFF since 2000 (Tokay et al. 2005). While the performance of optical, impact, and radar disdrometers and rain gauges were the main focus in early years, the vertically pointing radars, namely, MRR, and profiler were deployed to the site in June 2003 and October 2004, respectively, to study the microphysical characteristics of rainfall. WFF, located along the mid-Atlantic coast of the United States, receives an average of 98 cm of precipitation annually, with only a 3-cm difference between the months that receive the maximum and minimum precipitation. This even distribution of average rainfall through the annual cycle and variety of winter and summer precipitation make the site quite attractive for rainfall studies. However, the site is literally on the coast, and at times windy conditions have an effect on the measurements.

This study uses MRR, profiler, JW disdrometer and tipping-bucket gauges (Fig. 1). MRR is a 24-GHz frequency-modulated (FM) continuous wave (CW) Doppler radar. It has a small transmit power (50 mW), such that a common antenna is used for transmitting and receiving power and no beam overlapping occurs (Peters et al. 2005). MRR captures the Doppler spectra at each gate from which the raindrop size distribution (DSD) is retrieved under certain assumptions. Also, the two-way attenuation from the scattering volume is estimated from the retrieved DSD to adjust the 24-GHz returned power into Rayleigh scattering equivalent reflectivity factor. Therefore, the DSD-based derived rain parameters, such as reflectivity and rain rate, are subject to error. The two-way attenuation from the scattering volume was also calculated based on the retrieved DSD. Despite the MRRs shortcomings, Peters et al. (2005) showed a very good agreement in time series of rainfall derived from the lowest reliable MRR gates (100 and 300 m in their setup) and calculated from the DSD observed by surface impact and optical disdrometers. However, this was a light-to-moderate rain event, and a comprehensive study of comparison of the MRR and disdrometer reflectivity measurements in winter and summer storms has not been done.

The profiler is a pulsed Doppler radar operating at 2.835 GHz. It operates in two modes, sending out radar pulses with alternating lengths corresponding to range resolutions of 31 and 62 m every 7.5 s. This means that a full profile in both resolutions is retrieved every 15 s. For this study, the data were averaged over four cycles, so that the profiler matches both the MRR and the disdrometer observations (both are reported every minute). The profiler measures the vertical profile of reflectivity, Doppler fall speed, and its spectral width up to 6284 m at 31-m resolution and up to 12 485 m at 62-m resolution. The beamwidth is 3.2°, and the corresponding sample volume is 2332 m^3 at its third gate (177 m) at 31-m range resolution. The MRR, on the other hand, operates at 2° beamwidth, and the corresponding sample volume is 1029 m^3 at its fifth gate (175 m). Despite the profiler's sampling volume being more than twice the sampling volume of the MRR, we selected these heights (177 and 175 m) because of their closeness to compare their reflectivity measurements. The MRR and profiler (low mode) parameters are summarized in Table 1.

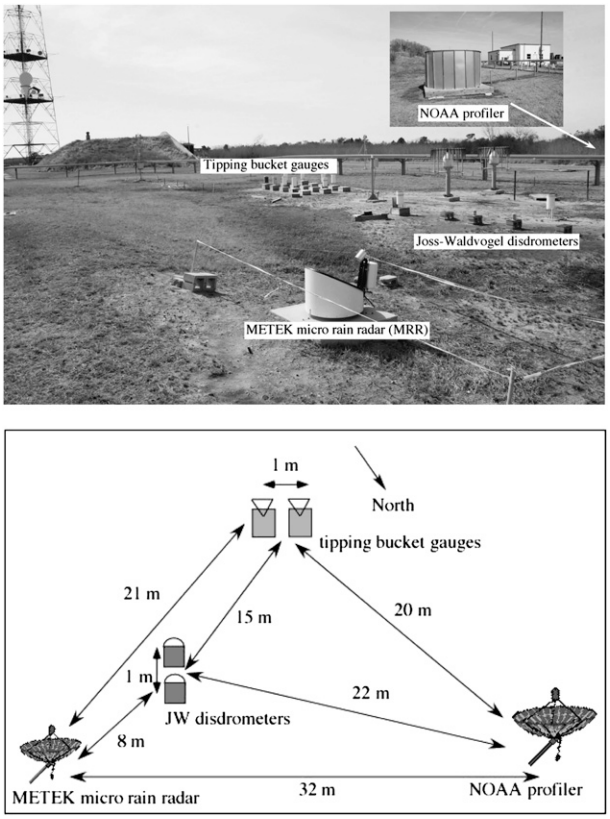

FIG. 1. (top) Picture of the site at NASA Wallops Flight Facility, and (bottom) the positions of the instruments with respect to each other.

The JW disdrometer measures the DSD by converting the impact of the falling hydrometeors to a drop diameter where the drops are assumed to fall at their terminal fall speed (Joss and Waldvogel 1967). In the presence of updrafts or downdrafts, the drop sizes are either underestimated or overestimated (Salles and Creutin 2003). The background noise suppresses the small drops. The small drops are also underestimated when two drops hit the sensor at the same time, known as dead time. This typically occurs at heavy rain (>10 mm h^{-1}). Electrical interference and windy conditions can also result in the underestimation of small drops (Donat Högl 2006, personal communication). The inability to distinguishing drops larger than 5-mm diameter

TABLE 1. Operating characteristics of MRR and profiler (low mode).

	MRR	Profiler (low mode)
Mean frequency	24 GHz	2835 MHz
Power	50 mW	380 W
Vertical range	35–1050 m	115–6284 m
Vertical resolution	35 m	31 m
Number of range gates	30	200
Averaging time	60 s	7.5 s
Beamwidth	2°	3.2°
Velocity range	0–12 m s^{-1}	−20–20 m s^{-1}

is another limitation of the instrument. In the presence of very large drops, this shortcoming can lead to the underestimation of rain parameters, particularly reflectivity, which is proportional to the sixth moment of the drop diameter. Nevertheless, the JW disdrometer provides very good results and has been widely used and compared with optical disdrometers (Tokay et al. 2001, 2002). The disdrometer used in this study was recently recalibrated by the manufacturer, and rain totals were compared with two reliable tipping-bucket rain gauges. We employed Met One Instrument tipping-bucket gauges, which have 0.01-in. resolution and a time stamp that is stored in a datalogger every second a tip occurs. The battery of the datalogger is routinely checked.

3. Rainfall statistics

A statistical package has been applied to paired variables represented by either event rain total or 1-min average reflectivity. The statistical package included the Pearson correlation coefficient ρ, which is the ratio of the sample covariance of the two variables (x and y) to the product of the two standard deviations and is expressed as

$$\rho = \frac{\mathrm{Cov}(x,y)}{[\mathrm{Var}(x)\mathrm{Var}(y)]^{1/2}}. \quad (1)$$

The Pearson correlation coefficient is neither robust nor resistant (Wilks 1995). It is not robust because a strong but nonlinear relationship between the two variables may not be recognized. It is not resistant because it is extremely sensitive to a single or a few outlying point pairs. Since a high correlation coefficient alone does not guarantee a good agreement between the paired variables, a low bias should also be satisfied. *Bias* is indicative of the position of paired variables with respect to the diagonal (one to one) line, and if one of the variables is taken as a reference, the bias indicates the underestimation or overestimation of the other variable. If the points were scattered at both sides of the one-to-one line, then the bias would be small but this does not guarantee good agreement in the absence of a high correlation coefficient. In this study, we defined the bias β between the two variables as

$$\beta = \frac{1}{n}\sum_{k=1}^{n}(x_k - y_k), \quad (2)$$

where n is the number of paired variables. The standard deviation of the difference (SD) between the two-paired variables provides a measure of the agreement between the two in terms of their distribution. Low standard deviation is one of the indications for the agreement between the considered paired of variables. The SD is expressed as

$$\mathrm{SD}(x-y) = \sqrt{\mathrm{Var}(x) + \mathrm{Var}(y) - 2\mathrm{Cov}(x,y)}. \quad (3)$$

If we consider one of the instruments as a reference, then we can calculate the measurement error of the second instrument. We employed absolute bias to quantify the measurement error of one of the instruments. The bias in Eq. (2) equally weights all the paired variables. Considering rainfall, the events that have higher accumulation have larger practical significance, as they can result in flooding. The weighted absolute bias $|\beta_w|$ is then calculated as

$$|\beta_w| = \sum_{k=1}^{n} w_k|(x_k - y_k)|, \quad (4)$$

where w_k is the weighting function and is calculated based on the reference instrument

$$w_k = \frac{x_k}{\sum_{k=1}^{n} x_k}. \quad (5)$$

Unlike the correlation coefficient, the last two statistics are not normalized and carry the units of the variables. Although the magnitude of the mean absolute difference between the two variables is important in rainfall, the percent absolute bias, a normalized quantity, is widely used in rainfall statistics. If variable x is considered to be a reference, the percent absolute bias $|\beta_{\mathrm{percent}}|$ becomes

$$|\beta_{\mathrm{percent}}| = \frac{\sum_{k=1}^{n}|(x_k - y_k)|}{\sum_{k=1}^{n} x_k}. \quad (6)$$

TABLE 2. Rain event table. The number of rainy minutes and maximum rain rate were provided based on JW disdrometer measurements, while both disdrometer and gauge 1 rainfall were included in the event totals. Not available (n.a.) indicates a disdrometer or gauge malfunction during segment or an entire period of a rain event. The disdrometer was substituted by a second unit for four consecutive events, which are highlighted by a superscript "2" next to the number of rainy minutes. The last column shows the availability for MRR, profiler, disdrometer, gauge 1, and gauge 2 in order. The labels 0, 1, and 2 mean not available, available, and partially available events, respectively.

	Start time (UTC)		End time (UTC)		No. of rainy minutes	Max rain rate (mm h^{-1})	Rain total (mm)		
Event no.	Day, month, year	Hour	Day, month, year	Hour	JW	JW	JW	Gauge 1	Availability
1	20 Oct 2004	0010	20 Oct 2004	0638	n.a.	n.a.	n.a.	32.5	12211
2	4 Nov 2004	1252	5 Nov 2004	0158	551	22.7	18.5	20.1	11111
3	10 Dec 2004	0212	10 Dec 2004	0456	133	74.8	20.7	22.4	11111
4	10 Dec 2004	0727	10 Dec 2004	1542	376	41.2	24.2	27.4	11111
5	10 Dec 2004	2242	11 Dec 2004	0013	89	85.2	25.5	26.9	11111
6	14 Jan 2005	1310	14 Jan 2005	2015	426	55.2	30.2	38.9	11111
7	30 Jan 2005	0500	30 Jan 2005	1654	672	5.6	15.3	21.8	11111
8	14 Feb 2005	0848	15 Feb 2005	0224	804	21.7	15.9	19.3	11111
9	1 May 2005	0508	1 May 2005	1426	353	13.9	10.3	9.7	01111
10	6 May 2005	0608	6 May 2005	2326	773	4.0	13.9	16.8	11111
11	20 May 2005	0453	20 May 2005	2046	573	76.2	36.7	38.9	11111
12	8 July 2005	0251	8 July 2005	1024	168	72.1	16.5	18.3	11111
13	9 Aug 2005	1911	10 Aug 2005	0135	211^2	79.8	14.5	11.4	11111
14	17 Aug 2005	0008	17 Aug 2005	0312	97^2	78.5	19.8	18.0	11111
15	19 Aug 2005	1558	20 Aug 2005	0034	355^2	38.7	33.6	32.0	12111
16	23 Aug 2005	1359	23 Aug 2005	2033	315^2	34.3	19.5	17.8	12111
17	18 Sep 2005	0221	18 Sep 2005	0246	21	90.3	14.1	n.a.	11100
18	7 Oct 2005	2107	8 Oct 2005	2223	958	73.7	55.1	n.a.	01100
19	21 Nov 2005	1159	22 Nov 2005	0603	941	24.1	33.4	39.1	11111
20	15 Dec 2005	1552	16 Dec 2005	0750	709	11.9	12.3	20.8	01110
21	25 Dec 2005	1438	26 Dec 2005	0105	233	42.4	15.1	15.0	11110
22	2 Jan 2006	2100	3 Jan 2006	0449	392	22.7	18.2	18.8	10110
23	14 Jan 2006	0648	14 Jan 2006	1222	173	46.1	11.4	13.2	11110
24	18 Jan 2006	1152	18 Jan 2006	1626	252	22.4	12.0	9.9	11110

4. Rain events

Through examining time series of disdrometer rainfall, we have determined 24 rain events that occurred between October 2004 and January 2006 (Table 2). All the events had at least 10 mm of rainfall, and any event that had mixed and/or frozen precipitation at the surface was excluded from this study. Consecutive rain events were separated based on the requirement that there were at least two hours of rain-free conditions between them. Interestingly, there were three rain events on 10–11 December 2004. Not all the instruments were available for all events. The MRR, for instance, was not available in three events, whereas the profiler data were missing in one event and were only partially available for another three events. Both rain gauges were not available for two rain events and one gauge was erroneous for the last five rain events. During August 2005, the JW disdrometer failed to operate (events 13–16), but fortunately a second JW disdrometer was available at the site and was used for that month. The JW disdrometer data were also partially missing during one event. Instrument failures are expected in field campaigns, and some instruments will vary in performance from one rain event to the next. Consequently, long-term (>1 yr) field campaigns involving multiple instruments are essential. The long-term field campaign at a midlatitude station is also advantageous to observe a vast variety of precipitation systems.

Since the rain statistics were applied to measurements obtained by instruments, time synchronization is an important factor. The instruments were logged on to different computers, but their clocks were periodically (from several days to a week) checked. Moreover, the time series of reflectivity between the radars and between the disdrometers was examined to determine any time shift.

Gauge 1, the reference instrument, accumulated 366 mm of rainfall in 16 rain events, which is just 5 mm more than gauge 2. The JW disdrometer, on the other hand,

collected 22 mm (8%) less rainfall than gauge 1. This was the period where both gauges and the JW disdrometer collected reliable data. Considering the event-by-event comparisons, the gauges had excellent agreement with high correlations and low biases (Fig. 2a). The percent absolute bias, for instance, was 4.4%. It should be noted that there was no wind fence around any instrument, and wind-induced undercatchment is a reality for in situ rain-measuring devices. Although special efforts including deployment of pit gauges have been made to demonstrate the wind effects on gauge performance in other studies (Duchon and Essenberg 2001; Sieck et al. 2007), this was not feasible for our site at Wallops Island. Despite the underestimation of rainfall by the JW disdrometer in most of the events, the agreement between gauge 1 and the disdrometer was very good (Fig. 2b). The percent absolute bias was 9.2%, well within the disdrometer manufacturer's specifications (Tokay et al. 2005).

5. Reflectivity comparisons

The profiler-measured, MRR-adjusted, and disdrometer-calculated Rayleigh reflectivities are compared with each other to demonstrate the agreement between the three instruments. The comparisons were performed for each event and by examining the vertical variations. The reflectivity in the Rayleigh regime is calculated from disdrometer DSD measurements as follows:

$$Z = \sum_{i=1}^{20} \frac{D_i^6 n_i}{v(D_i) t A}, \tag{7}$$

where D_i is the midsize diameter of the ith bin, n_i is the number of drops in ith bin, $v(D_i)$ is the terminal fall speed of the raindrops following Beard (1976), t is the sampling time (60 s), and A is the sampling cross section (0.005 m^2). The reflectivity is then converted from linear units ($mm^6\ m^{-3}$) to logarithmic units (dBZ), taking the logarithm in base 10 and multiplying by 10. As previously mentioned, MRR measures the reflectivity in the Mie regime and has built-in software that calculates the Rayleigh reflectivity through derived DSD parameters (Peters et al. 2005). The reflectivity in the Rayleigh regime is proportional to the sixth moment of drop diameter and is expressed as

$$Z = \int_0^\infty D^6 N(D)\, dD, \tag{8}$$

where $N(D)$ is the number of drops in unit volume in each dD size interval. For the rest of the manuscript, we refer to Raleigh reflectivity as reflectivity.

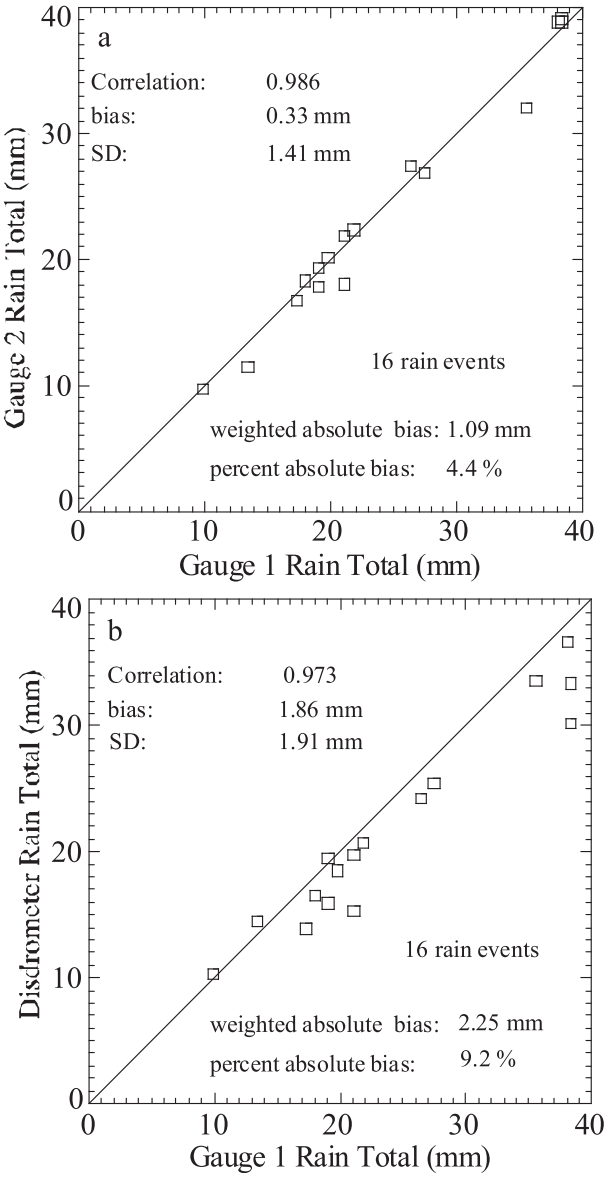

FIG. 2. Comparison of event rain totals (a) between the two collocated gauges, and (b) between a gauge and the disdrometer. The number of rain events and rainfall statistics are also given.

a. Rain event statistics

We compared the reflectivity measurements (in logarithmic units) by calculating the correlation, the bias, and the SD using (1), (2), and (3), respectively. For the profiler and the MRR, we selected their third and fifth gate, respectively, where the center heights are at 177 and 175 m, respectively. The radar sample volumes were similar, with the profiler sample volume of 2322 m^3 being a little more than 2 times as large as the MRR's as a result of the wider beamwidth, as noted in section 2. In contrast, although the disdrometer sampling volume over a minute

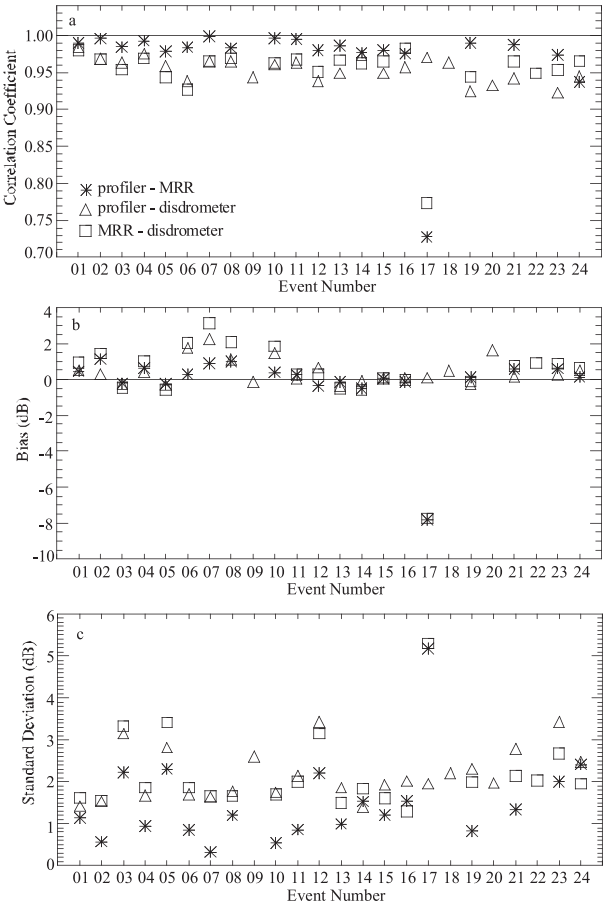

FIG. 3. Event-by-event comparison of reflectivity between profiler (third gate) and MRR (fifth gate), (∗); between profiler (third gate) and disdrometer, (△); and between MRR (fifth gate) and disdrometer, (□). (a) The correlation coefficient, (b) bias, and (c) SD were presented to demonstrate the agreement between the instruments.

varied by drop size, it was at least four orders of magnitude smaller than the S band's sampling volume.

Overall, the agreement between the radars and the disdrometer was good. Ignoring event 17, the intense convection event where the MRR results seem spurious (perhaps due to attenuation), the event correlation coefficients for either radar versus the disdrometer ranged between 0.92 and 0.98 (Fig. 3a). Given their overlapping and similarly sized sample volumes, the agreement between the profiler and the MRR was even better, with 18 of the 19 events having correlation coefficients higher than 0.97. Similarly, the fluctuations of event biases show more precise agreement with radar-to-radar than radar-to-disdrometer comparisons (Fig. 3b). In particular, the radar-to-radar event bias (profiler less MRR) fluctuated roughly between −0.5 and 1 dB, while the radar-to-disdrometer bias (radar less disdrometer) ranged between −0.7 and 3 dB. The SD of observed reflectivity difference between either radar and the disdrometer ranged between 1.4 and 3.4 dB, while the SD of the typically smaller differences between the profiler and the MRR ranged roughly between 0.2 and 2.4 dB (Fig. 3c).

These statistics are consistent with the relatively good agreement between radars and disdrometer measurements, as reported previously by Gage et al. (2004). Tokay et al. (2005) studied the agreement between six collocated JW disdrometers for eight events and the root-mean-square difference (RMSD) range was between 1.4 and 3.6 dB, much higher than the range found here between the profiler and the MRR. We attribute this result to the differences in sampling volume between radar and disdrometer platforms. The variability of rainfall estimates can be expected to be inversely proportional to the sampling volumes, regardless of the platform used. Indeed, Habib et al. (2001a) found higher correlations between gauges when the gauge data were averaged for longer periods of time. Here, the agreement between the larger volumes of radars was better than the agreement between the "point" measurements of disdrometers.

b. Vertical variability

The time–height ambiguity between the radar and disdrometer measurements has been studied by comparing the correlation coefficient, bias, and SD for the matched pairs of reflectivity in logarithmic units. We merged the events where all three instruments were operating, but we excluded event 17 because of MRR failure. We considered all 30 gates of the MRR and the first 32 heights for the profiler, and we made sure that both radars were reporting at all heights. The maximum heights for the MRR and for the profiler were 1050 and 1076 m, respectively, which were below the bright band for all the events. This resulted in 6201 samples. The mean statistics for each height level was calculated by applying a weighting based on the sample size of each event (Fig. 4). To demonstrate the variability of statistics between the different events, we calculated the 95% confidence intervals. The 95% confidence interval refers to the second lowest and second highest events when the event statistics were sorted from the lowest to the highest value. No time shift was applied between the radar and disdrometer observations at this stage, but it was considered later in the study (section 7).

An examination of the statistics between the radar and disdrometer reflectivities confirmed that the second gate of the radars is the first reliable gate; therefore, we eliminated the first gates from further analysis and discussion. For the profiler–disdrometer pair, the correlation coefficient ranged between 0.95 and 0.77,

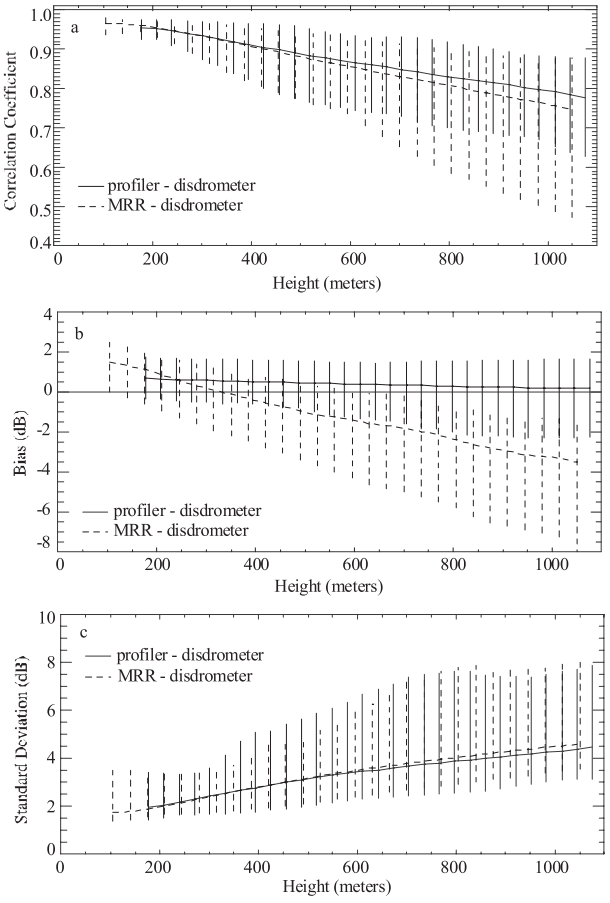

FIG. 4. Comparison of reflectivity between profiler and disdrometer (solid line) and between MRR and disdrometer (dashed line) as a function of height within rain layer. The vertical bars represent the 95% confidence interval of the event-based (a) correlation coefficient, (b) bias, and (c) SD.

peaking at the profiler's third gate (177 m), then gradually decreasing with height (Fig. 4a). For the MRR–disdrometer pair, the highest correlation coefficient occurred at the third gate of the MRR (105 m) and the correlation decreased with height, in the range between 0.96 and 0.74. The agreement in correlation coefficient between the two pairs was excellent at altitudes below 500 m, but the MRR–disdrometer pair had relatively lower correlations at higher heights. Although increased sampling volume differences between the two radars may play a role, the error associated with the retrieved MRR reflectivity is believed to be a leading cause for the differences in correlations. The range of confidence intervals broadened with height in the MRR–disdrometer pair in all three statistics as well.

The high correlations were accompanied with low biases (Fig. 4b) in profiler–disdrometer comparisons but not in MRR–disdrometer comparisons. Although the profiler minus disdrometer bias was always less than 1 dB regardless of height, the MRR minus disdrometer bias ranged from 1.7 dB at the MRR's second gate to −3.5 dB at the MRR's highest gate. It crossed zero bias at around the 10th gate (350 m). The absolute value of the bias between the MRR and the disdrometer was less than 1 dB between the MRR 6th (210 m) and 14th (490 m) gate. Since the correlation decreased with height, the low correlations were accompanied with higher absolute biases above the 14th gate of the MRR.

The SD between the radars and the disdrometer pairs had an increasing trend with increasing separation. For the profiler–disdrometer pair, the SD was lowest at the profiler's third gate and increased with height, ranging between 1.9 and 4.5 dB (Fig. 4c). For the MRR–disdrometer pair, the lowest SD occurred at the MRR's third gate (105 m) and increased with height, ranging between 1.8 and 4.6 dB. As for the correlation coefficient, the SD between the two pairs had an excellent agreement at heights below 500 m, and the SD of the MRR–disdrometer pair was slightly higher at higher levels. We again attributed the differences in SD comparisons to the errors in reflectivity retrieval in the MRR. The main contribution to reflectivity is from midsize (1–3-mm diameter) and large (>3-mm diameter) drops, and the errors in retrieval of the DSD from the Doppler spectra at these sizes results in erroneous reflectivity, particularly in convective storms where ignored air velocities are not negligible. Since the results presented here imply that the MRR is reliable only up to 500 m, the MRR-retrieved reflectivities above this height are eliminated from further analysis and discussion.

The time–height ambiguity between radar and disdrometer measurements was further investigated by grouping matched pairs of profiler and disdrometer observations at five different reflectivity intervals. These 1-dB-wide reflectivity intervals were centered at 20, 25, 30, 35, and 40 dBZ (based on the disdrometer-calculated reflectivity) and represented light, light-to-moderate, moderate, moderate-to-high, and high reflectivity, respectively. The bias was positive and either 1 dB or less at 20, 25, and 30 dBZ, indicating relatively higher readings of profiler measurements (Fig. 5a). At 35 dBZ, the bias was negative except for a few profiler gates near the ground. At this reflectivity interval, the magnitude of the bias exceeded 1 dB above 700 m but never exceeded 1.5 dB. The bias at the 40-dBZ interval was also mainly negative except near the ground. The magnitude of the bias increased with height, reaching 4 dB at 1076 m (the highest profiler height). The SD gradually increased with height from 2 dB to just above 4 dB for the first four reflectivity intervals (Fig. 5b). At the 40-dBZ interval, the SD rapidly increased with height, reading 7 dB at the profiler's highest height.

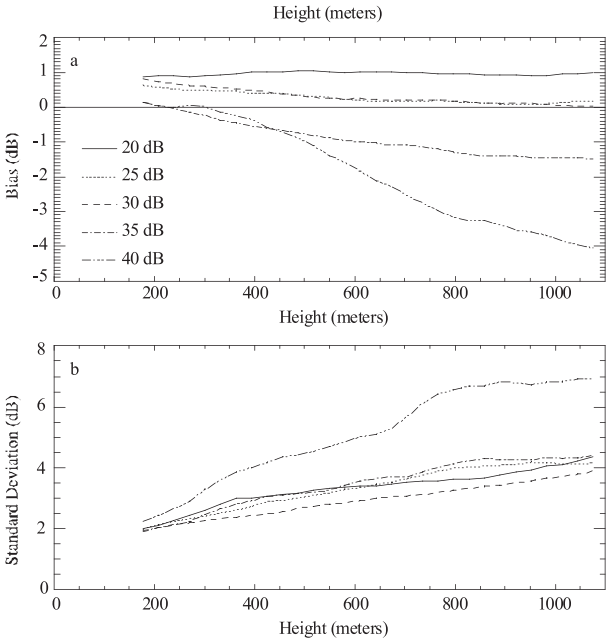

FIG. 5. Comparison of reflectivity between profiler and disdrometer as a function of height at selected (disdrometer calculated) reflectivity regimes. The (a) bias and (b) SD are calculated between profiler and disdrometer reflectivities.

Since the DSD is typically wider at high reflectivity, drop sorting between the large and small drops is more pronounced at this reflectivity range, providing a possible explanation for these observations.

6. *Z–R* relations

The variability of the *Z–R* relations with height is examined through disdrometer and vertically pointing radar measurements. Operationally, the NWS employs five different *Z–R* relations that are optimum for summer deep convection, tropical deep convection, stratiform, and winter stratiform precipitation east and west of the Continental Divide. In mathematical form, *Z–R* relation is traditionally expressed as

$$Z = AR^b, \tag{9}$$

where A and b are the coefficients and are referred to as *coefficient* and *exponent*, respectively. Since Z is the measured and R is the estimated variable, the relation is actually derived in reverse order ($R = A'Z^{b'}$) and then converted to Eq. (9) where $A = (1/A')^{(1/b')}$ (and $b = (1/b')$. Coefficients and exponents in operational *Z–R* relations range between 75 and 300 and between 1.2 and 2.0, respectively. These *Z–R* relations are for rain only and are applied by NWS officers to the lowest tilt of radar observations to obtain storm totals (Fulton et al. 1998).

a. Vertical variability

The vertical variability of the *Z–R* relation has its practical significance at far ranges of the radar measurements. For instance, the WSR-88D intersects 1 km above the ground at around 90 km from the radar at its lowest tilt, and radar rainfall maps can extend up to 230 km. In that regard, we derived *Z–R* relations by applying linear least squares fit to profiler reflectivity and disdrometer rainfall for 31 profiler gates between 146 and 1076-m height with no time shift. We then repeated the same exercise by employing adjusted MRR reflectivities for its 13 gates between 70 and 490 m. The linear least squares is a linear regression between ln(Z) and ln(R), where ln(Z) is a dependent variable and ln(R) is an independent variable; it has been widely used in the literature (e.g., Pani and Jurica 1989).

Prior to the derivation of the *Z–R* relation, we combined the above-mentioned 19 storms and will refer to the corresponding relation as *climatological Z–R*. Considering the storm-to-storm variability of the precipitation systems, we derived *Z–R* relations for each event and then took the average and the 95% confidence interval of coefficients and exponents. The latter derived relation is referred to as *event average Z–R*. It should also be noted that there is also variability between convective and stratiform regimes of the same storm (e.g., Tokay and Short 1996), but this was not considered here.

Considering the profiler-based *Z–R* relations, the coefficient decreased and the exponent increased with height (Figs. 6a,b). The coefficient of climatological *Z–R* was higher than the event average *Z–R*, while the vice versa is true for the exponent of the *Z–R* relations. The difference in coefficient and exponent between the two relations also increased with height. The 95% confidence interval had a wide variability of coefficient and exponent, indicating strong storm-to-storm variability. For the coefficient, it was about 350 and steady with height, whereas for the exponent, it increased with height from 0.4 to 0.8. Considering the default NWS $Z = 300R^{1.4}$ relation, which is best suited for summer convection, the coefficient was always within the 95% confidence interval range of this study, whereas the exponent fell out of the confidence interval at altitudes above 250 m.

Considering MRR-based *Z–R* relations, the coefficient decreased with height, whereas the exponent was first steady and then gradually increased with height (Figs. 6c,d). Unlike the profiler-based *Z–R* relations, there were no difference between climatological and event average *Z–R* relations in either coefficient or exponent. Looking at the 95% confidence of the MRR–

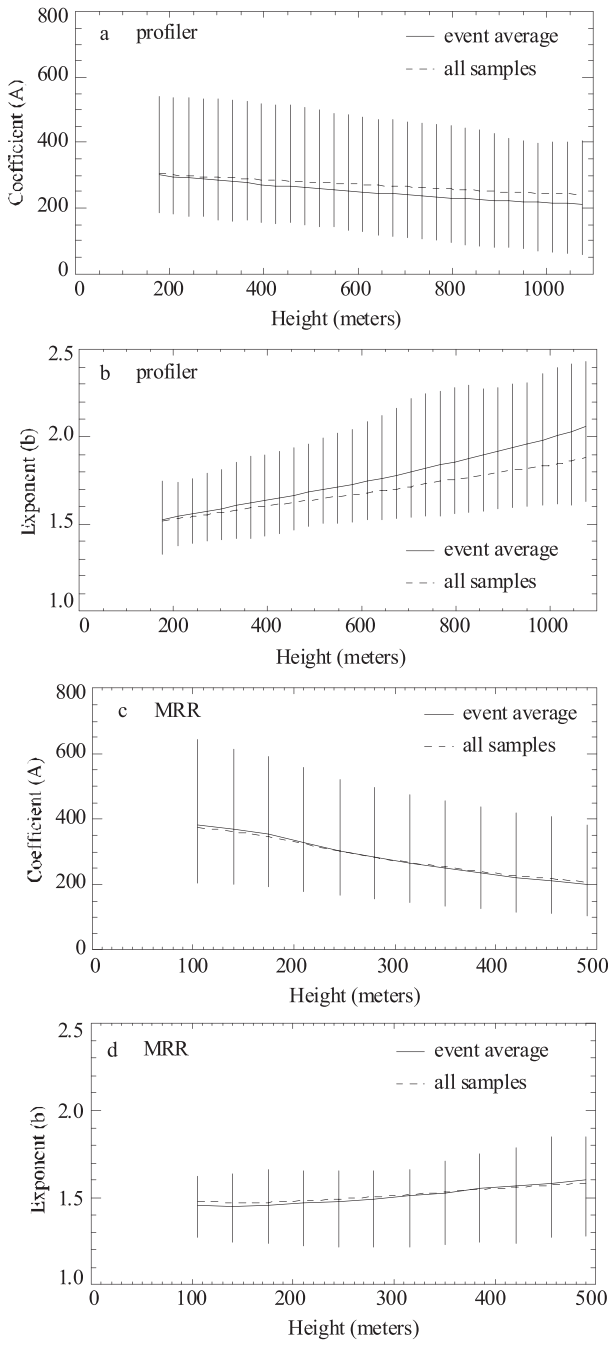

FIG. 6. Vertical variation of the (a),(c) coefficient and (b),(d) exponent of the Z–R relations based on (top) profiler or (bottom) MRR reflectivity and disdrometer rain rate. The linear least squares fit was applied to the combined dataset of 6201 samples (curves) as well as to individual events to derive Z–R relations. The vertical bars represent 95% confidence intervals of the parameters of event-based Z–R relations.

disdrometer-based Z–R relations, the coefficient decreased with height from about 450 to 300, whereas the exponent increased with height from 0.3 to 0.6. Both the coefficient and exponent of the default NWS $Z = 300R^{1.4}$ relation were within the range of MRR–disdrometer-based Z–R relations.

The profiler- and MRR-based climatological Z–R relations were compared by interpolating the coefficient and the exponent of the relations for the heights between 150 and 500 m, as shown in the first two columns of Table 3, where the linear fit method was used. The exponent was higher for the profiler–disdrometer pair for all heights, while the coefficient was higher for the MRR–disdrometer pair at 250 m and below. The Z–R relation was also derived from the disdrometer measurements, as shown in Table 3b. The exponent of the disdrometer Z–R relation was either equal or slightly lower than that of the profiler- and MRR-based Z–R relations at 150 m, while the coefficient of the disdrometer Z–R relation was substantially lower than that for the coefficient of the profiler- and MRR-based Z–R relations at the same height. This means that the disdrometer Z–R relation results in higher rainfall regardless of the reflectivity regime. For the rest of this paper, we considered 20, 30, and 40 dBZ as typical values that represent light, moderate, and high reflectivity regimes, respectively. The differences in coefficient and exponent of profiler–disdrometer- and MRR–disdrometer-based Z–R relations also imply substantial differences in rainfall estimates.

- At *low reflectivity*, a rainfall increase with height is implied by both relations, but a profiler-based Z–R produces higher rainfall below 250 m.
- At *moderate reflectivity*, a rainfall increase with height is implied from the MRR-based Z–R, while rainfall from the profiler-based Z–R did not show any vertical variation.
- At *high reflectivity*, a rainfall increase with height is implied from MRR-based Z–R, while a rainfall decrease with height is implied by the profiler-based Z–R. The rainfall implied by the profiler-based Z–R was higher at only at 150 m. More importantly, the difference in rain estimates between the profiler- and MRR-based Z–R increased with height reaching 2.8 mm h^{-1} (24%) at 500 m.

b. Sensitivity to the method of derivation

The Z–R relations discussed above were derived based on the linear least squares fit method. The parameters of the Z–R relations that were derived from the linear and nonlinear least squares fits result in substantial differences (e.g., Ciach and Krajewski 1999; Campos and Zawadzki 2000; Tokay et al. 2001). Moreover, both methods result in bias in rain estimates. Steiner and Smith (2000, 2004) discussed the nonunique features of least square fits and implemented two additional

TABLE 3a. The coefficient (A) and exponents (b) of the Z–R relations that were derived from profiler–disdrometer and MRR–disdrometer pairs of measurements. The parameters were interpolated to the heights between 150 and 500 m with a 50-m increment.

Height (m)	Profiler linear	MRR linear	Profiler nonlinear	MRR nonlinear	Profiler PMM	MRR PMM	Profiler bias-adjust	MRR bias-adjust	Profiler min-RMSD	MRR min-RMSD
150	323, 1.49	356, 1.47	169, 1.70	556, 1.14	338, 1.37	371, 1.36	279, 1.49	270, 1.47	340, 1.50	478, 1.18
200	303, 1.53	330, 1.48	180, 1.67	436, 1.20	317, 1.40	346, 1.35	252, 1.53	245, 1.48	328, 1.49	440, 1.19
250	297, 1.55	299, 1.49	186, 1.65	350, 1.24	313, 1.40	314, 1.35	241, 1.55	216, 1.49	327, 1.49	348, 1.24
300	294, 1.57	274, 1.51	177, 1.67	280, 1.30	312, 1.40	291, 1.35	231, 1.57	192, 1.51	331, 1.49	254, 1.33
350	290, 1.59	254, 1.53	176, 1.67	247, 1.32	309, 1.40	272, 1.34	220, 1.59	172, 1.53	329, 1.49	250, 1.32
400	285, 1.61	235, 1.55	175, 1.67	208, 1.37	307, 1.40	253, 1.34	209, 1.61	153, 1.55	324, 1.49	209, 1.37
450	282, 1.62	219, 1.57	282, 1.68	190, 1.38	306, 1.40	238, 1.34	200, 1.62	139, 1.57	328, 1.49	185, 1.39
500	278, 1.64	202, 1.59	278, 1.69	170, 1.40	303, 1.40	222, 1.33	191, 1.64	124, 1.59	325, 1.49	173, 1.39

methods: (1) the exponent of the linear least squares was fixed but the coefficient varied until the bias between the Z–R-based and the disdrometer (true) rainfall was zero for a given rain event, and (2) both parameters of the Z–R relation varied until the RMSD between the Z–R-based and true rainfall was minimum for a given rain event. In addition to the linear and nonlinear least squares fits (methods 1 and 2), we implemented these two methods but for the merged rain events (methods 3 and 4). We used the probability matching method (PMM) as the fifth method (Rosenfeld et al. 1993, 1994; Amitai 2000). The PMM generates radar reflectivity versus rain rate table by matching the equal percentiles of the probability density functions of radar reflectivity and gauge rain rate. The table includes pairs that either or both radar and gauge report rainfall. The PMM does not yield a Z–R relation. In this study, we employed vertically pointing radar and disdrometer matched pairs, with both instruments reporting rainfall, and we applied linear least squares fit on the matched pairs to retrieve coefficients and exponents. Therefore, there is a difference in the original and our PMM methods.

For the profiler-based climatological Z–R relations, the minimum RMSD resulted in the highest coefficient followed by the PMM and linear fits. The coefficients of these three methods did not show substantial variability with height (Fig. 7a). The coefficient of bias-adjusted fit, on the other hand, decreased with height and merged with nonlinear fits at heights above 800 m. The nonlinear fit has the lowest coefficient, and the maximum difference of the coefficient between the five methods increased with height from 175 to 235. The exponent of the PMM was the lowest followed by minimum RMSD, and they both are almost invariant with height (Fig. 7b). The exponent of the linear fit increased with height, crossing the exponent of the nonlinear fit near 800 m. The exponent of the nonlinear fit was the largest below 800 m. The maximum difference of the exponent between the four methods was 0.3 and uniform at heights below 600 m and increased to 0.5 above that height.

For the MRR-based climatological Z–R relations, the coefficients of bias-adjusted, linear, and PMM fits gradually decreased with height, where bias-adjusted fits had the lowest and PMM fits had the highest coefficient among these three relations (Fig. 7c). The coefficients of the nonlinear and minimum RMSD methods agreed well with each other, decreasing sharply, crossing the coefficients of PMM and linear fits at 280 m and then gradually decreasing at higher heights. The maximum difference of coefficient between the five methods was as high as 400 at the MRR's lowest reliable gate, but it decreased to 100 at 280 m and did not change at higher heights. Unlike the exponent of linear fit, the exponent of the PMM fit gradually decreased with height (Fig. 7d). Since the former were higher than the latter, the difference between the two also increased with height. Similar to the coefficients, the exponents of nonlinear and minimum RMSD agreed well with each other. They increased with height until 320 m and were rather uniform at higher heights. The maximum difference of the exponent between the four methods was between 0.3 and 0.4.

The choice of method resulted in drastic differences in both coefficients and exponents for the profiler- and MRR-based Z–R relations, as shown in Table 3a. The coefficients and exponents of the disdrometer Z–R relations shown in Table 3b were also different from

TABLE 3b. The coefficient and exponents of disdrometer-derived Z–R relations.

Method	A	b
Linear	266	1.47
Nonlinear	190	1.58
PMM	271	1.42
Bias adjusted	251	1.47
Min RMSD	190	1.58

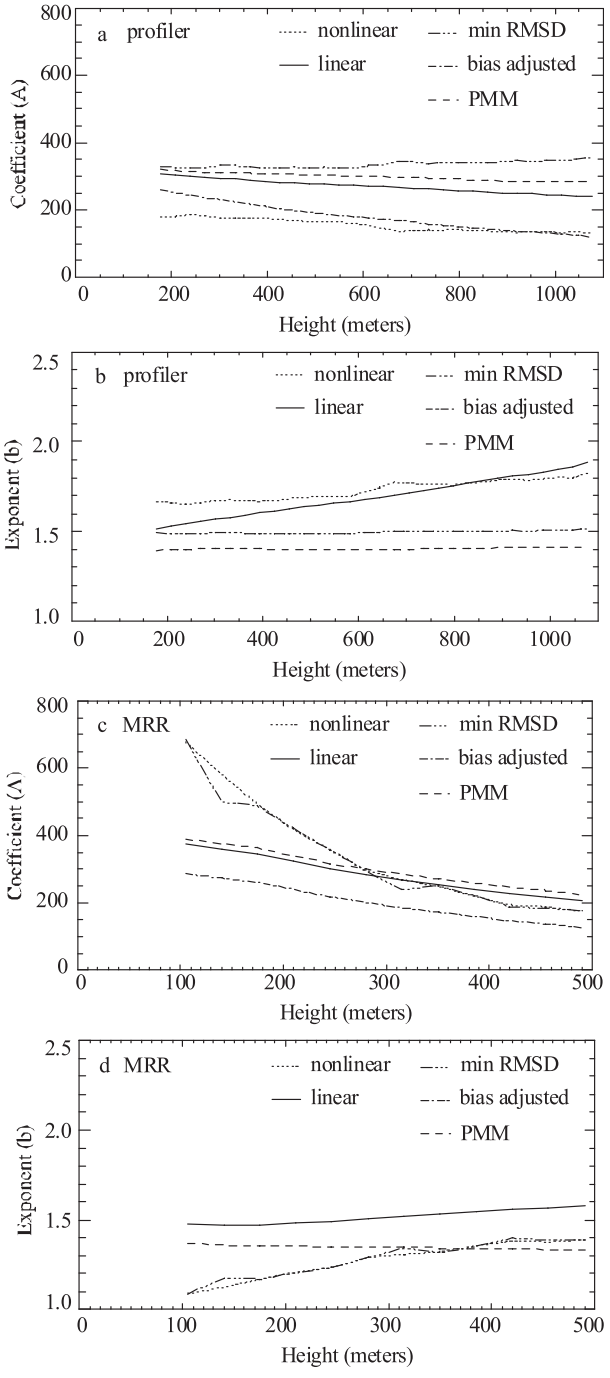

FIG. 7. Vertical variation of the (a),(c) coefficient and (b),(d) exponent of the Z–R relations based on (a),(b) profiler or (c),(d) MRR reflectivity and disdrometer rain rate. The curves represent five different methods of derivation of the Z–R relations.

radar-based Z–R relations. These differences imply substantial differences in derived rainfall at low, moderate, and high reflectivity regions. Nevertheless, the differences in rainfall as a result of the different methods of derivation were less than those due to the profiler- and MRR-based Z–R relations.

- At *low reflectivity*, the nonlinear and PMM fits imply a maximum rainfall difference for profiler-based Z–R relations at 150 m. The difference in rainfall was 0.3 mm h^{-1} (45%) and was less than 0.5 mm h^{-1} (70%) between profiler- and MRR-based Z–R relations when nonlinear fit was employed at the same height.
- At *moderate reflectivity*, the implied rainfall difference reached 0.7 mm h^{-1} (25%) when nonlinear and linear fits were used in profiler-based Z–R relations at 150 m. The nonlinear fit weights the heavy rainfall more and therefore exhibits larger differences at light and moderate rain intensities.
- At *high reflectivity*, the differences in implied rainfall are more noticeable at higher heights. At 500 m, the PMM and linear fits resulted in 3.3 mm h^{-1} (27%) difference in profiler-based Z–R relations. Although the occurrence of high reflectivity is much less than that of the low and moderate reflectivities, the choice of method results in large differences in rain amounts, which in turn, can play a significant role in radar rain estimation.

7. Time lag

As stated in the introduction, the drop sorting is one of three sources for the mismatch between the radar measurements aloft and the rain gauge and disdrometer measurements at the surface. This drop sorting contributes to a decorrelation with altitude of the distribution of drops in a sampling volume. If the mean diameter of the size distribution is 1 mm, then it will take 4.48 min for a drop of this size to reach the ground from 1076 m with a terminal velocity of 4 m sec^{-1}. Similarly, the same drop will reach the ground at 2.04 min if it is falling from 490 m. The reader should be reminded that these are the highest altitudes of profiler and MRR that were considered in this study. The smaller drops (<1-mm diameter) reach the ground at longer time steps, whereas the reverse is true for the larger drops. An updraft would slow the vertical motion of the drops as well. To quantify this effect, we examined the RMSD of reflectivity between the radars and disdrometer measurements by adding time shifts of 1–4 min to the disdrometer measurements. The minimum RMSD prevailed for zero time lag up to 394 and 420 m for the profiler–disdrometer and the MRR–disdrometer pairs, respectively (Figs. 8a,b). Although the variation in the minimum RMSD between the 1- and 2-min lags was similar with height, the 1-min lag still resulted in the

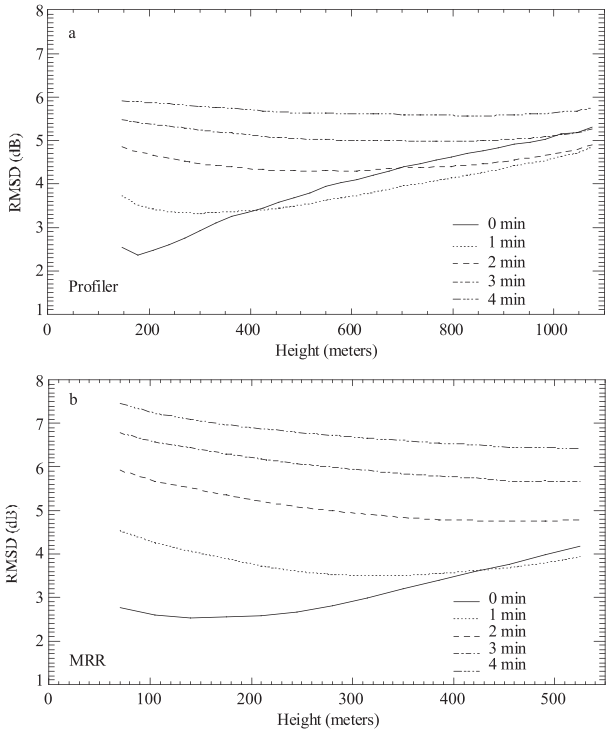

FIG. 8. Comparison of reflectivity between (a) profiler and disdrometer and (b) between MRR and disdrometer measurements as a function of height when no time lag and 1–4 min between the observations of two instruments time lag were considered. The RMSD was presented to show the agreement between the instruments.

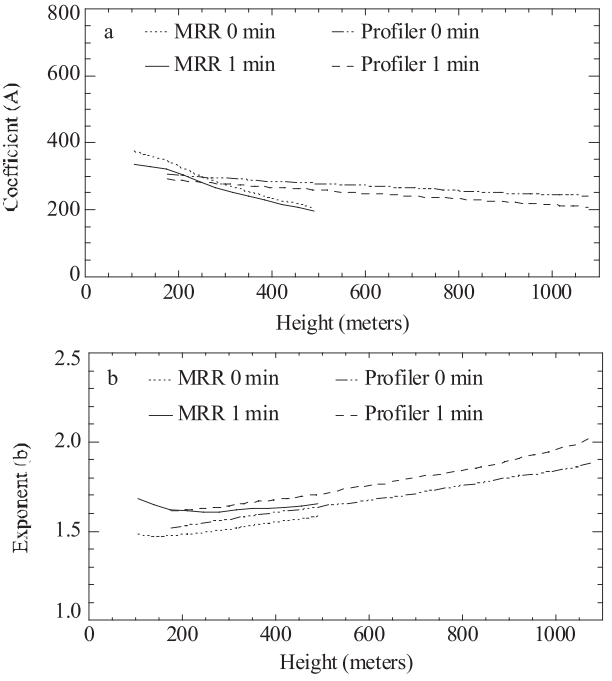

FIG. 9. Vertical variation of (a) coefficient and (b) exponent of the Z–R relations based on profiler or MRR reflectivity and disdrometer rain rate when no time lag and 1-min time lag between the observations of the two instruments were considered.

lowest RMSD at all remaining heights in profiler–disdrometer and MRR–disdrometer pairs.

We then examined the role of the time lag in parameters of the Z–R relations by comparing 1-min time lag with 0 time lag datasets. For that, we employed linear least squares and combined all of the events. The coefficient of Z–R relations was lower, whereas exponent was higher when the 1-min time lag is considered (Figs. 9a,b). The difference between coefficients between 1-min and 0 time lag gradually increased with height, reaching 33 at 1076 m in profiler-based Z–R relations. The MRR-based Z–R relations, on the other hand, had a relatively greater difference in the coefficient. It decreased with height and had a difference of 11 at 420 m. The exponent of the profiler-based Z–R relations did not show a significant change with height and reached its maximum difference of 0.14 at 1076 m. The MRR-based Z–R relations, on the other hand, had relatively higher differences in the exponent at lower heights and the exponent had a difference of 0.07 at 420 m.

The role of time lag on the rain estimate implied by the Z–R relation was then examined for low, moderate, and high reflectivities. At low reflectivity, the difference in rain rate was 0.07 mm h^{-1} (10%) at 1076 m for profiler-based Z–R relations and 0.03 mm h^{-1} (5%) at 420 m for MRR-based Z–R relations. The difference in rain rate was either the same or even lower at moderate reflectivity. At high reflectivity, the rain rate difference was 0.45 mm h^{-1} (6%) at 1076 m for profiler-based Z–R relations and 0.89 mm h^{-1} (8%) at 420 m for MRR-based Z–R relations. Overall, the time lag did not seem to play a major role in Z–R-relation-based rain rate estimation.

8. Conclusions

A unique dataset of long-term observations of collocated disdrometer, and K- and S-band vertically pointing radars were employed to investigate the time–height ambiguity between radar measurements aloft and disdrometer measurements at the surface.

The event-by-event comparison of disdrometer-calculated, MRR-calculated, and profiler-measured reflectivities showed the effect of sample volume size. The agreement between the MRR and profiler reflectivities was better than that between each radar and the disdrometer. Comparison of similar statistics between the profiler and MRR reflectivities in conjunction with a comparison from a previous study (Tokay et al. 2005)

of collocated disdrometer reflectivities suggests that the agreement seems to be better between the larger volumes, although the overlap in radar volumes likely also plays a role.

The poorer agreement between the disdrometer and radar reflectivities, especially at higher heights, is largely a result of the spatial separation of the sample volumes. Moreover, the disagreement between platforms was significantly greater at high reflectivity when paired disdrometer and profiler measurements were stratified based on reflectivity. The higher bias and lower correlations between paired MRR and disdrometer reflectivities than between paired profiler and disdrometer reflectivities suggests attenuation, and the assumptions in retrieved size distribution compromised MRR reflectivity calculations. Since the bias between paired MRR and disdrometer reflectivities exceeded 1 dB around 500 m, we disregarded MRR measurements above this height. The user is cautioned for the quantitative use of MRR above half a kilometer.

Considering reflectivity magnitude dependence of the time–height ambiguity, the absolute value of the bias between profiler and disdrometer reflectivity exceeded 1 dB above 600 and 500 m at 35 and 40 dB, respectively, and increased with height. Thus, the agreement between profiler and disdrometer was systematically reduced with increasing height at moderate-to-high intensities. Among the many factors that can contribute to this decrease in agreement are drop sorting and wind, which will contribute to decorrelation in the distribution of raindrops in the profiler sampling volume with changes in height.

The decreased agreement between the profiler and disdrometer reflectivity at moderate-to-high intensities is a concern for radar rainfall estimates in regions where the operational gauges are sparse. From the measurement site at Wallops Island down to the tip of Delmarva Peninsula, for instance, the distance to the closest WSR-88D is more than 90 km, and the gauge coverage in this region is considered to be poor. Given that the lowest elevation angle of the WSR-88D crosses 500 m at about 44-km range, the operational rainfall products, such as NOAA's multisensor precipitation estimator (MPE), may not be able to produce an accurate precipitation estimate in the southern Delmarva region. The MPE is a product that merges rainfall measurements from rain gauges, and rain estimates from WSR-88Ds and Geostationary Operational Environmental Satellite (GOES) products (Xie et al. 2005).

Considering the vertical variability of the Z–R relation, the coefficient A decreased and the exponent b increased with height. The 95% confidence interval of event average Z–R relations showed the highly variable nature of the storm-to-storm variability. Since the rain rate is taken from disdrometer measurements, the vertical variability of Z–R relations is mainly linked to the vertical variability of reflectivity. Given that the midsize and large drops are the main contributors to the reflectivity, the DSD in these size regimes at a lower altitude differs from DSD at a higher altitude within the measured volume. For operational use, the single Z–R-based radar rainfall estimate can therefore have high error margins at mid-to-long ranges and at moderate-to-heavy rainfall. The presence of gauges at these radar ranges is particularly important for the gauge adjustment.

While the sensitivity of the Z–R relation to the method of derivation has been shown, the linear least square is vastly used in the literature. In this study, we explore this further by deriving profiler–disdrometer pair climatological Z–R relations for five different methods. Although bias-adjusted and minimum RMSD methods result in no bias in rain estimate and are therefore advantageous, it was not our intension to recommend any particular method of derivation. Rather, this study demonstrates how the coefficients of Z–R relations and retrieved rainfall change when the relation was derived from different methods.

Regarding time lag between reflectivity measurements aloft and rain rate measurement at the surface, the minimum RMSD between radar and disdrometer reflectivity measurements prevailed for zero time lag at around 400 m. Then, the 1-min lag resulted in the lowest RMSD at all remaining heights. The resultant variability in the coefficient and the exponent of the derived Z–R relations between zero lag and 1-min lag was marginal and therefore did not result in significant differences in rain rate.

Acknowledgments. This study was initiated and mostly conducted during Peter Hartmann's visit to the NASA Goddard Space Flight Center, and we are thankful to the Joint Center for Earth System Technology, the University of Maryland Baltimore County, the Meteorological Institute at the University of Bonn (particularly to Clemens Simmer), and the NASA Goddard Space Flight Center for providing financial and logistic support. Thanks also go to Richard Lawrence of the NASA Goddard Space Flight Center and John Gerlach of the NASA Wallops Flight Facility for their leadership in ground validation efforts of the TRMM program, which supports the instrumentation at the NASA Wallops Flight Facility. The micro rain radar has been operated through an agreement with METEK, led by Hans-Jürgen Kirtzel and Lutz Hirsch. Paul E. Johnston and David Carter of NOAA/ Earth Systems Research Laboratory shared responsibilities in installation, upgrading, and data transfer of the profiler. Discussions with Robert

Meneghini of the NASA Goddard Space Flight Center; George Huffman, Brad Fisher, David Marks, and Jianxin (Jerry) Wang of Science Systems Applications Inc. and the NASA Goddard Space Flight Center; and Emad Habib of University of Louisiana-Lafayette were very helpful. We would like to acknowledge the anonymous reviewer, Walter A. Petersen of the Marshall Space Flight Center, and Eyal Amitai of Chapman University for their efforts in reviewing our manuscript. This study was supported by NASA's TRMM program through Grant NAG5-13615 under Ramesh Kakar, program scientist. The work of P. Hartmann and A. Battaglia has been supported by the German Science Foundation in the frame of the Transregio T32 project Pattern in Soil–Vegetation–Atmosphere–Systems: Monitoring, Modeling and Data Assimilation.

REFERENCES

Amitai, E., 2000: Systematic variation of observed radar reflectivity–rainfall rate relations in the tropics. *J. Appl. Meteor.,* **39,** 2198–2208.

Beard, K. V., 1976: Terminal velocity and shape of cloud and precipitation drops aloft. *J. Atmos. Sci.,* **33,** 851–864.

Campos, E., and I. Zawadzki, 2000: Instrumental uncertainties in *Z–R* relations. *J. Appl. Meteor.,* **39,** 1088–1102.

Ciach, G. J., 2003: Local random errors in tipping-bucket rain gauge measurements. *J. Atmos. Oceanic Technol.,* **20,** 752–759.

——, and W. F. Krajewski, 1999: Radar–rain gauge comparisons under observational uncertainties. *J. Appl. Meteor.,* **38,** 1519–1525.

Clark, W. L., K. S. Gage, C. R. Williams, and A. Tokay, 2005: The importance of cross validation in climate studies: Selected case studies of radar/disdrometer reflectivity comparisons. Preprints, *13th Symp. on Meteorological Observations and Instrumentation*, Savannah, GA, Amer. Meteor. Soc., 5.3. [Available online at http://ams.confex.com/ams/pdfpapers/93839.pdf.]

Duchon, C. E., and G. R. Essenberg, 2001: Comparative rainfall observations from pit and aboveground rain gauges with and without wind shields. *Water Resour. Res.,* **37,** 3253–3263.

Fulton, R. A., J. P. Breidenbach, D.-J. Seo, D. A. Miller, and T. O'Bannon, 1998: The WSR-88D rainfall algorithm. *Wea. Forecasting,* **13,** 377–395.

Gage, K. S., C. R. Williams, P. E. Johnson, W. L. Ecklund, R. Cifelli, A. Tokay, and D. Carter, 2000: Doppler radar profilers as calibration tools for scanning radars. *J. Appl. Meteor.,* **39,** 2209–2222.

——, W. L. Clark, C. R. Williams, and A. Tokay, 2004: Determining reflectivity measurement error from serial measurements using paired disdrometers and profilers. *Geophys. Res. Lett.,* **31,** L23107, doi:10.1029/2004GL020591.

Habib, E., W. F. Krajewski, and G. J. Ciach, 2001a: Estimation of rainfall interstation correlation. *J. Hydrometeor.,* **2,** 621–629.

——, ——, and A. Kruger, 2001b: Sampling errors of fine resolution tipping-bucket rain gauge measurements. *J. Hydrol. Eng.,* **6,** 159–166.

Joss, J., and A. Waldvogel, 1967: Ein spectrograph für Niederschlasgstropfen mit automatischer Auswertung (A spectrograph for the automatic analysis of raindrops). *Pure Appl. Geophys.,* **69,** 240–246.

Lee, G., and I. Zawadzki, 2005: Variability of drop size distributions: Noise and noise filtering in disdrometric data. *J. Appl. Meteor.,* **44,** 634–652.

Pani, E. A., and G. M. Jurica, 1989: A *Z–R* relation for summertime convective clouds over West Texas. *J. Appl. Meteor.,* **28,** 1081–1088.

Peters, G., B. Fischer, H. Munster, M. Clemens, and A. Wagner, 2005: Profiles of rain drop size distributions as retrieved by microwave radars. *J. Appl. Meteor.,* **44,** 1930–2005.

Rosenfeld, D., D. B. Wolff, and D. Atlas, 1993: General probability-matched relations between radar reflectivity and rain rate. *J. Appl. Meteor.,* **32,** 50–72.

——, ——, and E. Amitai, 1994: The window probability matching method for rainfall measurements with radar. *J. Appl. Meteor.,* **33,** 682–693.

Salles, C., and J.-D. Creutin, 2003: Instrumental uncertainties in *Z–R* relationships and raindrop fall velocities. *J. Appl. Meteor.,* **42,** 279–290.

Sieck, L. C., S. J. Burges, and M. Steiner, 2007: Challenges in obtaining reliable measurements of point rainfall. *Water Resour. Res.,* **43,** W01420, doi:10.1029/2005WR004519.

Steiner, M., and J. A. Smith, 2000: Reflectivity, rain rate, and kinetic energy flux relationships based on raindrop spectra. *J. Appl. Meteor.,* **39,** 1923–1940.

——, and ——, 2004: Scale dependence of radar-rainfall rates—An assessment based on raindrop spectra. *J. Hydrometeor.,* **5,** 1171–1180.

Tokay, A., and D. A. Short, 1996: Evidence from tropical raindrop spectra of the origin of rain from stratiform versus convective clouds. *J. Appl. Meteor.,* **35,** 355–371.

——, A. Kruger, and W. F. Krajewski, 2001: Comparison of drop size distribution measurements by impact and optical disdrometers. *J. Appl. Meteor.,* **40,** 2083–2097.

——,——,——, P. Kucera, and A. J. Pereira Filho, 2002: Measurements of drop size distribution in the southwest Amazon basin. *J. Geophys. Res.,* **107,** 8052, doi:10.1029/2001JD000355.

——, P. G. Bashor, and K. R. Wolff, 2005: Error characteristics of rainfall measurements by collocated Joss–Waldvogel disdrometers. *J. Atmos. Oceanic Technol.,* **22,** 513–527.

Wilks, D. S., 1995: *Statistical Methods in the Atmospheric Sciences: An Introduction*. Academic Press, 467 pp.

Williams, C. R., K. S. Gage, W. Clark, and P. Kucera, 2005: Monitoring the reflectivity calibration of a scanning radar using a profiling radar and a disdrometer. *J. Atmos. Oceanic Technol.,* **22,** 1004–1018.

Xie, H., X. Zhou, E. R. Vivoni, J. M. H. Hendrickx, and E. E. Small, 2005: GIS-based NEXRAD Stage III precipitation database: Automated approaches for data processing and visualization. *Comput. Geosci.,* **31,** 65–76.